



RESEARCH ARTICLE **OPEN ACCESS**

# RNA-Seq and ChIP-Seq Identification of Unique and Overlapping Target Genes and Pathways Regulated by TBX4 in Human Pulmonary Fibroblasts and Pericytes

Ying Cai<sup>1</sup> | Ling Yan<sup>1</sup>  | Joy D. Cogan<sup>1</sup> | Lora K. Hedges<sup>2</sup> | Bethany Nunley<sup>1</sup> | Nick Negretti<sup>3,4,5</sup> | Jennifer M. S. Sucre<sup>3,4,5</sup> | James West<sup>6</sup>  | Eric D. Austin<sup>2</sup> | Rizwan Hamid<sup>1</sup>

<sup>1</sup>Division of Medical Genetics and Genomic Medicine, Vanderbilt University Medical Center, Nashville, Tennessee, USA | <sup>2</sup>Division of Allergy, Immunology, and Pulmonary Medicine, Vanderbilt University Medical Center, Nashville, Tennessee, USA | <sup>3</sup>Mildred Stahlman Division of Neonatology, Vanderbilt University Medical Center, Nashville, Tennessee, USA | <sup>4</sup>Department of Cell and Developmental Biology, Vanderbilt University, Nashville, Tennessee, USA | <sup>5</sup>Department of Pediatrics, Biodevelopment Origins of Lung Disease (BOLD) Center, Nashville, Tennessee, USA | <sup>6</sup>Division of Allergy, Pulmonary, and Critical Care Medicine, Department of Medicine, Vanderbilt University Medical Center, Nashville, Tennessee, USA

**Correspondence:** James West ([j.west@vumc.org](mailto:j.west@vumc.org))

**Received:** 3 September 2024 | **Revised:** 13 January 2025 | **Accepted:** 7 February 2025

**Funding:** The study is supported by the National Heart, Lung, and Blood Institute (P01 HL 108800, R01 HL 102020, R01 HL095797, and R01 HL134802) and Cardiovascular Medical Research and Education Fund.

**Keywords:** ChIP-seq | extracellular matrix (ECM) | pulmonary arterial hypertension (PAH) | RNA-seq | T-Box 4 (TBX4)

## ABSTRACT

Transcription factor *TBX4* rare variants associate with pulmonary arterial hypertension (PAH), particularly in children, and are the second most common cause of heritable PAH. However, *TBX4*'s down-stream targets and the molecular and cellular pathways these targets regulate remain largely unknown in PAH. We combined RNA-seq and ChIP-seq results to identify *TBX4* direct targets in lung fibroblasts and pericytes, respectively. There were 555 genes with altered expression with *TBX4* knock-down in both fibroblasts and pericytes by RNA-seq, and which also were found to be bound by *TBX4* by ChIP-seq. Gene ontology analysis found that these were dominated by genes related to extracellular matrix, actin organization, and migration guidance, although there were also significant groups related to serine/threonine kinase signaling, GTPase mediated signaling, and glycoprotein metabolism. Migration and proliferation studies using *TBX4* knockdown fibroblasts confirmed functional effects. These studies provide the first insights into how genes and pathways regulated by *TBX4* are impacted and inform future studies about the key biological processes that lead to PAH in patients who carry pathologic *TBX4* rare variants.

## 1 | Introduction

*T-box4* (*TBX4*) is a member of the T-box transcription factor family. Expressed in the developing atrium of the heart, limb buds, and lung mesenchyme trachea [1], *TBX4* plays a significant role during embryogenesis. Rare heterozygous single nucleotide variants (SNVs) or copy number variant (CNV) deletions in *TBX4* have been associated with parenchymal

lung diseases of variable severity, ranging from lethal neonatal developmental lung diseases (e.g., acinar dysplasia and congenital alveolar dysplasia) to milder forms of parenchymal growth abnormalities. More recently, *TBX4* variants have associated with idiopathic and hereditary pulmonary arterial hypertension (IPAH/HPAH) particularly in children, making *TBX4* the second most common of heritable PAH cause [2–12]. While it has been shown that *TBX4* regulates FGF10,

Eric D. Austin and Rizwan Hamid contributed equally to senior authorship of this manuscript.

This is an open access article under the terms of the [Creative Commons Attribution-NonCommercial](https://creativecommons.org/licenses/by-nc/4.0/) License, which permits use, distribution and reproduction in any medium, provided the original work is properly cited and is not used for commercial purposes.

© 2025 The Author(s). *Pulmonary Circulation* published by John Wiley & Sons Ltd on behalf of Pulmonary Vascular Research Institute.

BMP-SMAD1/5, and SHH-FOXF1 pathways [9, 13, 14], the molecular mechanisms of its role in PAH pathogenesis remain unclear.

Our primary objective in this study was to identify direct *TBX4* binding targets, with a secondary goal of unraveling the downstream transcriptional cascades it initiates. To achieve this, we employed chromatin immunoprecipitation sequencing (ChIP-Seq). Because ChIP-Seq is known to have a high false positive rate [15, 16], we enhanced the reliability of our data by performing ChIP-seq on two distinct cell types, and focused on genes bound by *TBX4* in both. Additionally, we conducted RNA-seq on these cell types with and without *TBX4* knock-down, enabling us to correlate differential gene expression with *TBX4* binding sites identified by ChIP-Seq. This integrated approach allowed us to pinpoint downstream *TBX4* targets and map the transcriptional networks regulated by *TBX4*.

## 2 | Materials and Methods

### 2.1 | Cell Lines

The human lung pericyte cell line (HLPC) was kindly provided by Hongkuan Fan, PhD. Primary early human lung fibroblasts (HLF) were generated in 2018 and frozen as previously described [17]. HEK293FT and HLF were maintained in recommended medium: Dulbecco's Modified Eagle Medium (Merck KGaA, Darmstadt, Germany) supplemented with 10% FBS (Merck KGaA, Darmstadt, Germany), 1 mM sodium pyruvate, 1% streptomycin/penicillin and 4 mM L-glutamine (Gibco Thermo Fisher Scientific, Waltham, MA USA). HLPC were plated on 0.2% gelatin-coated dishes in human Pericyte Medium (ScienCell Research Laboratories, Carlsbad, CA, USA).

### 2.2 | Single-Cell RNA-Sequencing Analysis

Data from single-cell RNA sequencing in lung tissue samples were analyzed for marker gene expression in different lung cell types as previously reported [18]. This previously published data set was generated from a mouse lung cellular suspension that was depleted of Ter119 + blood cells and CD45 + immune cells and sequenced using the 10× Genomics Chromium platform. For this analysis, data from mesenchymal cells at E12, E15, E18, P0, P3, P5, and P7 mice were interrogated for *Tbx4* expression and reported as a function of each previously defined mesenchymal cell population and developmental timepoint.

### 2.3 | Plasmids and Cell Transfection

Plasmids encoding shRNA targeted to *TBX4* and *TBX4* siRNA were ordered from Thermo Fisher Scientific (Waltham, MA, USA). For *TBX4* shRNA vectors, Clone IDs are TRCN0000432100 and TRCN0000415957, for *TBX4* siRNA, cat# is s18203. For *TBX4* knockdown (KD) in HLF by *TBX4* siRNA, cells were plated at a density of  $1.8 \times 10^6$  cells/plate in a 10 cm plate, and then transfected with 150 pmol *TBX4* siRNA or control siRNA by Lipofectamine RNAiMAX reagent (Invitrogen Thermo Fisher

Scientific, Waltham, MA, USA) following the manufacturer's instructions. For HLPC retrovirus-mediated *TBX4* shRNA infection, cells were treated with polybrene (6 µg/mL), a cation polymer used to increase the efficiency of infection, and incubated at 37°C for 20 min, then lentiviral particles packaging *TBX4* shRNA or control scramble shRNA were added to medium and incubated for 24 h. Lentivirus-infected HLPC were selected by puromycin 16.66 µg/mL, and viable cells were expanded into a 75 cm<sup>2</sup> flask and used for subsequent experiments.

### 2.4 | Retrovirus Packaging

Lentiviral packaging vectors psPAX2 and pMD2.G were co-transfected into HEK293FT cells with the vector encoding shRNA targeted to *TBX4*, or with the control vector pLKO.1. After 48 h, media was harvested, spun at 1250 rpm for 5 min, and the supernatant filtered through a 0.45 µm filter to remove the cells. Virus supernatant was frozen at -80°C for long-term storage until use.

### 2.5 | Western Blot, RNA Isolation, Reverse Transcription, and Quantitative Real-Time Polymerase Chain Reaction (RT-qPCR)

The *TBX4* antibody for Western Blot was sc-398903 (F-12) (Santa Cruz Biotechnology, Dallas, TX USA). RNA was isolated using the RNeasy Mini kit from QIAGEN. Reverse transcription followed the iScript cDNA Synthesis kit protocol (Bio-Rad). All quantifications utilized standard curve real-time PCR.

### 2.6 | RNA-Seq and ChIP-Seq

*TBX4* Chromatin immunoprecipitation was done using the EZ-Magna ChIP A/G kit (Merck-Millipore, Burlington, MA USA). Chromatin was Cross-linked by 1% formaldehyde, then was sheared to approximately 300–1000 bp fragments using a Bioruptor Sonicator (Diagenode, Denville, NJ USA) with the following pulse mode settings: 30 s with 30 s cooling, high power, 12 cycles. DNA/protein complexes were immunoprecipitated overnight using an anti-*TBX4* antibody NBP1-32879 (Novus Biologicals, Centennial, CO USA). Rabbit IgG antibody (Merck-Millipore, Burlington, MA USA) was used as a negative control. Protein-DNA immune complexes and input DNA (cross-linked and sonicated but not immunoprecipitated sample) were decross-linked, and deproteinized according to the manufacturer's protocol. DNA was extracted using a spin filter column (Merck-Millipore, Burlington, MA USA). The sequencing of RNA-seq and ChIP-seq were done by Vanderbilt University Medical Center, Vantage lab (Nashville, TN USA).

### 2.7 | Bioinformatic Analyses of RNA-Seq and ChIP-Seq Data, and Pathway Analyses

ChIP-Seq analysis was performed by Basepair (New York, NY USA). In brief, raw reads were aligned to human genome release 19 by Bowtie2, and counts of alignments to specific

genes and gene locations (promoter; exon; intron; intergenic) performed using HOMER2 (Hypergeometric Optimization of Motif EnRichment) [19].

Bulk RNA-Seq were analyzed using Partek. In brief, raw reads were aligned to human genome release 38 using Hisat2, then quantified to the Hg38 annotation model using Partek E/M, and counts normalized to counts per million. RNA-seq data is available at Geo (<https://www.ncbi.nlm.nih.gov/geo/>) as accession number GSE273499. Pathway analyses were done by the Reactome pathway analysis tool (<https://reactome.org>) and by Webgestalt (<https://www.webgestalt.org>).

### 3 | Results

#### 3.1 | RT-PCR Results Confirm That TBX4 Is Mainly Expressed in Lung Fibroblasts and Pericytes

We queried a single cell (sc) RNAseq atlas of the developing mouse lung [18]. The results showed that TBX4 is expressed in

mesenchyme, with negligible expression in the epithelium or endothelium. Within the mesenchyme, TBX4 showed high expression levels in myofibroblasts and pericytes, while its expression in smooth muscle cells was relatively lower. Peak expression was observed at embryonic Day 18 in myofibroblasts, and postnatally in pericytes (Figure 1A).

We then compared *TBX4* expression in HLPC, HLF, pulmonary arterial smooth muscle cells (PASMC), and pulmonary microvascular endothelial cells (PMVEC) by RT-PCR analysis. *TBX4* had the highest expression in HLF and HLPC, relatively lower expression levels in PASMC. PMVEC had very low *TBX4* expression (Figure 1B). The RT-PCR data corroborated the findings from the mouse lung scRNA-seq, indicating that *TBX4* is predominantly expressed in mesenchymal cells (fibroblasts and pericytes) within the lung. Its expression is lower in smooth muscle cells and minimal in endothelial cells.

We also confirmed localization of *TBX4* transcription in tissue sections in postnatal Day 7 (P7) lungs using RNAScope (Figure 1C). Note that at P7, a majority of the cells in the lungs are still mesenchyme, as the process of alveolarization is

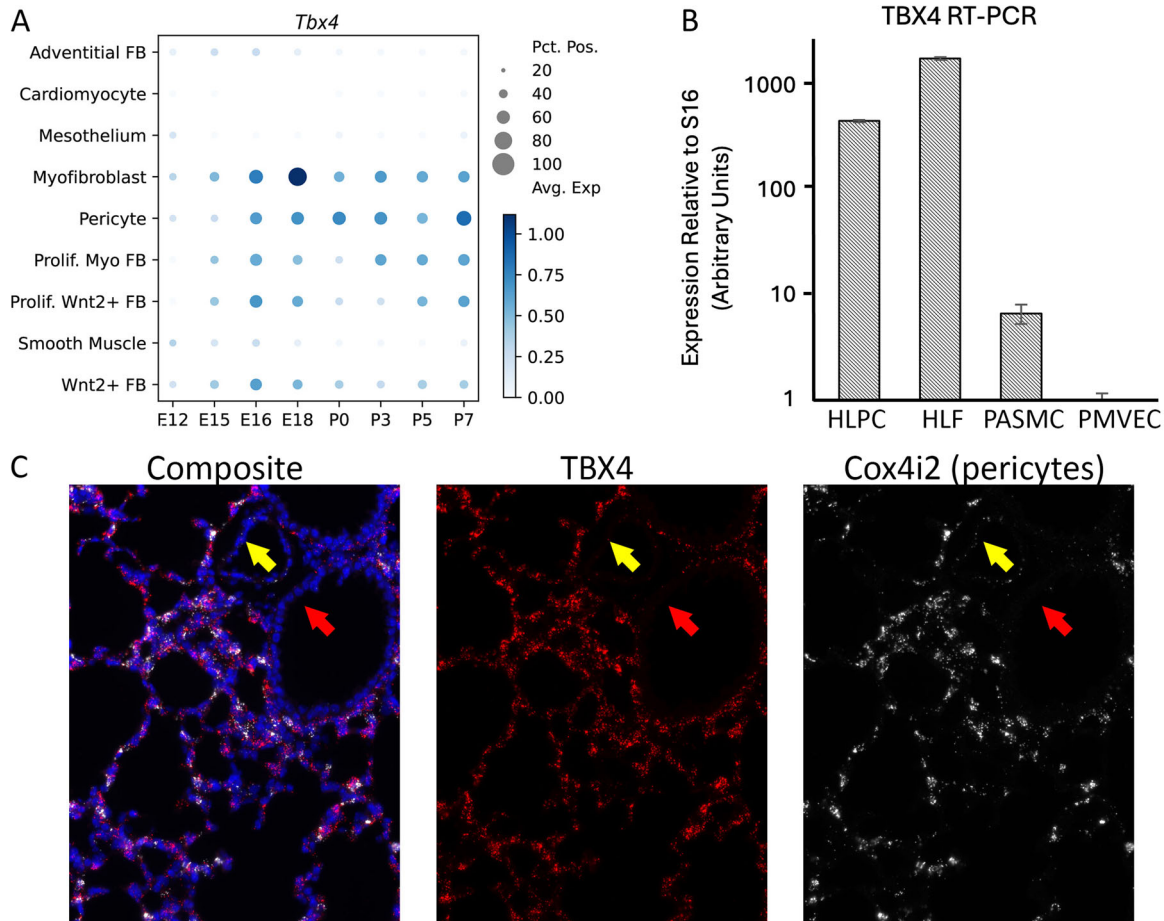


**FIGURE 1** | TBX4 is primarily expressed in myofibroblasts and pericytes. (A) TBX4 expression levels from a single cell RNA-seq atlas. Dot color is indicative of expression level; size is percent of cells expressing TBX4 within that category; labels are different cell types, including five sub-categories of fibroblast. (B) RT-PCR results demonstrate that TBX4 is mainly expressed in mesenchymal origin cell lines—highest in early human lung fibroblasts (HLF) and pericytes (HLPC), lower in smooth muscle (PASMC), lowest in endothelial cells (PMVEC). (C) RNA-Scope shows location of TBX4 RNA (red dots) and the pericyte marker Cox4i2 (white dots) with DAPI nuclear stain (blue) at postnatal Day 7. Red arrows are to draw attention to an epithelial ring (negative); yellow arrow indicates a blood vessel, likely primarily endothelium (also negative). At P7, much of the alveolar space is still mesenchyme, which we would expect to be positive. RT-PCR, real-time polymerase chain reaction.

ongoing, where we would expect varying levels of TBX4 expression. However, there is a clear airway (red arrow) with adjoining blood vessel (yellow arrow) in this image in which TBX4 is absent, confirming TBX4 is not expressed meaningfully in epithelium, endothelium, or smooth muscle.

### 3.2 | TBX4 RNA-Seq in Lung Fibroblasts and Pericytes

As the dominant sites of expression, we focused on human lung fibroblasts (HLF) and human lung pericytes (HLPC) for the rest of this study. Although there was some level of expression in smooth muscle cells, it was > 10x lower than in HLPC, and 100x lower than in HLF. Moreover, while most PH is thought of as a consequence of defective vascular function [20], where the role of PASMC is critical, data both from human patients [21] and from initial mouse studies [22] suggest that the impact of TBX4 mutation is primarily on pulmonary vascular development.

To elucidate the function of TBX4 in the lung, we knocked down TBX4 in human lung fibroblasts (HLF) and human lung pericytes (HLPC), and performed RNA-seq on the resulting cells. TBX4 was knocked down 2.1x in HLF and 4.3x in HLPC, as assessed by RNA-seq. Functional knockdown of TBX4 was also demonstrated by the fact that cells with TBX4 knockdown are separated from control cells by principal components analysis on the RNA-seq data (Figure 2A).

In fibroblasts, 13567 genes have average expression above 1 count per million (CPM). Of these, 4485 protein-coding genes have altered expression by TBX4 knockdown at  $p < 0.05$ , and 1594 of these genes are altered at  $p < 0.01$  (Supporting Information: Table 1A). Two hundred and four of these are changed more than 2x. In pericytes, 14,158 genes have average expression above 1 CPM. Of these, 3662 genes are altered at  $p < 0.05$ , and 1703 are altered with  $p < 0.01$  (Supporting Information: Table 1B). 343 of these are changed more than 2x. 1309 genes are regulated at  $p < 0.05$  in both fibroblasts and pericytes, or 244 at  $p < 0.01$ . Gene ontology overrepresentation analysis was performed on the 552 protein-coding genes with  $p < 0.05$  of a minimum fold change of 1.2x in both pericytes and fibroblasts. Ontology groups with a multiple comparisons-modified false discovery rate of below 0.05 included many with clear relevance to the known phenotype of TBX4 knockout. These included taxis, vascular development, inflammatory response, mesenchyme response, and calcium regulation, among others (Figure 2B). Some of the groups in the ontology analysis are somewhat spurious—for instance, neuron projection is probably only there because many genes related to taxis are altered.

Even those genes that are regulated in common between fibroblasts and pericytes often move in opposite directions between the two cell types. Figure 2C depicts genes from the extracellular matrix gene ontology group that are significantly changed in both pericytes and fibroblasts. Roughly half move in the opposite direction in the two cell types. This lack of coherency doesn't necessarily indicate that these are spurious results; transcription factor actions often are very dependent on both cell type and other contexts [23–25].

### 3.3 | TBX4 Chip-Seq in Lung Fibroblasts and Pericytes

ChIP-Seq combined with data analysis can be used to identify the binding sites and the target genes of DNA-associated proteins. Figure 3A shows the workflow of ChIP-seq and following data analysis. To detect TBX4 direct targets in lung fibroblasts and pericytes, we carried out TBX4 ChIP-seq analysis in HLF and HLPC. After data normalization, 27,314 and 44,846 strongly-enriched binding sites with about 300-bp peak size for HLF and HLPC, respectively were detected (Supporting Information: Table 2A and 2B are TBX4 ChIP-seq results for HLF and pericyte, respectively). Those binding sites are annotated to transcription start site (TSS), the genomic locations of enriched peaks of TBX4 in HLF and HLPC showed a similar wide distribution pattern (Figure 3B). Among the 27,314 enriched peaks detected for TBX4 in HLF, 8641 different genes were identified; Similarly, 44,846 TBX4 binding sites in HLPC were annotated to 9908 different genes. The TBX4 binding motifs in HLF and HLPC were generated from overrepresented DNA peaks and analyzed for similarity to known binding motifs (Supporting Information: Table 3A and 3B).

### 3.4 | Combined RNA-Seq and Chip-Seq to Identify Targets, Pathways Regulated by TBX4 in Lung Fibroblasts and Pericytes

We compared targets found in RNA-seq results of early HLF and HLPC with their corresponding ChIP-seq results. We found that there in HLF were 2178 genes with both altered expression in TBX4 knockout cells, and which were identified as a potential binding site in the ChIP pulldown. The corresponding number for HLPC was 2181 (Figure 4A). The two cell types had 555 genes in common; these genes are differentially regulated by TBX4 in both HLF and HLPC, and included putative TBX4 binding sites in both cell types as well. Supporting Information: Table 4A–C are TBX4 direct targets in HLF, in HLPC and the common targets respectively.

To determine pathways regulated by TBX4 in HLF and HLPC, we used Webgestalt ([www.webgestalt.com](http://www.webgestalt.com)), using a Bonferroni multiple comparisons-adjusted false discovery rate (FDR) of 0.05 or less. We found 10 nonredundant overrepresented gene ontology groups (Figure 4B, Table 1; additional details in Supporting Information: Table 5A). Including potentially overlapping/redundant sets, there were 69 sets including 324 of the 555 genes with  $FDR < 0.05$  (Supporting Information: Table 5B).

The most significant groups in the GO analysis are all related to cell motility; actin filament-based process and extracellular structure organization includes a variety of genes related to cell migration (substantially the same as those plotted in Figure 3B; specific lists of genes are included in Supporting Information: Tables 5A and 5B). Although the actual name of the “neuron projection guidance” group is probably inappropriate to the setting, the actual genes in this group include, for instance, several semaphorins, which are known to be directional cues for both vascular [26] and alveolar [27] growth and repair.



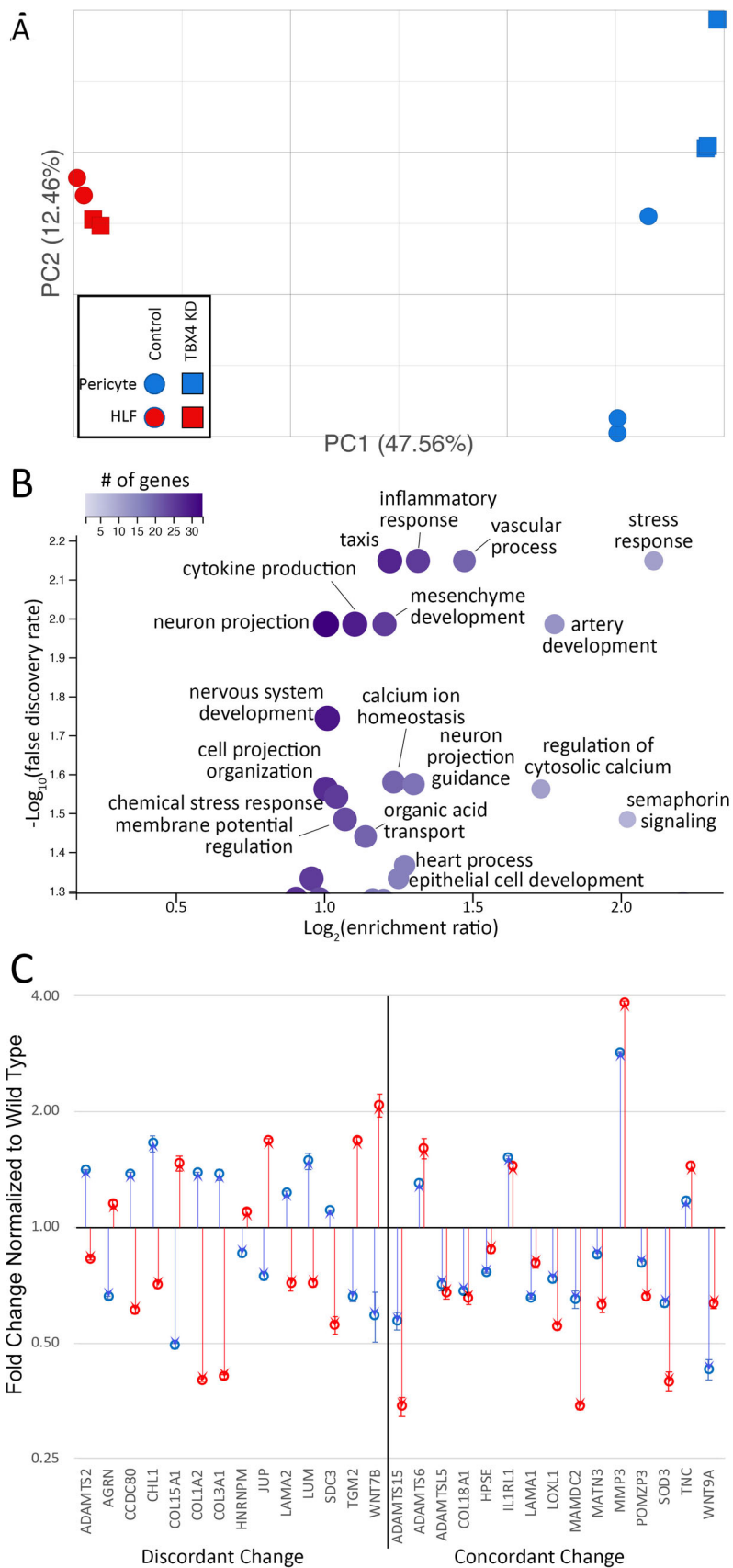
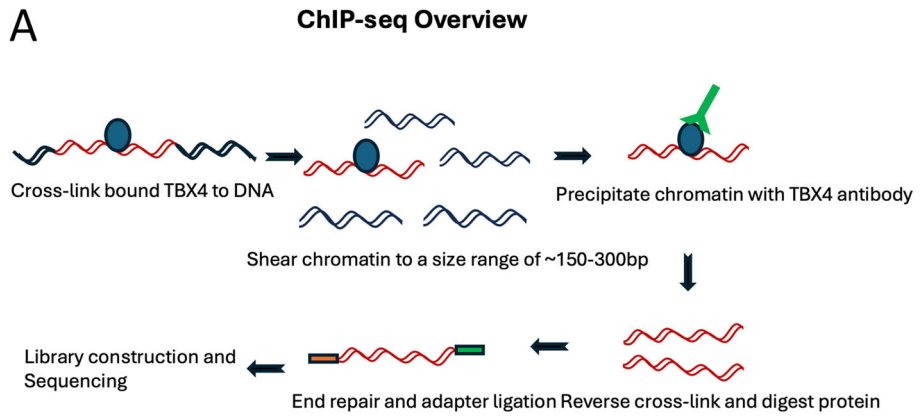
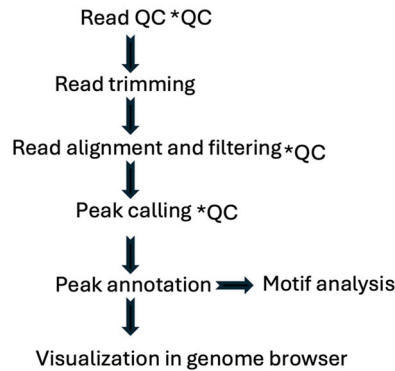


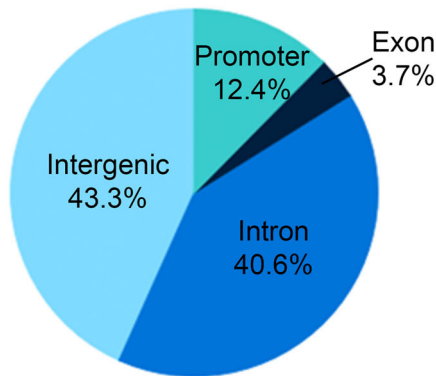
**FIGURE 2** | RNA-seq outcomes. (A) Principal components analysis. HLF and HPC are well separated, and control and TBX4 knockdown are separated; the direction of separation is distinct in HLF and HPC, indicating different effects in the two cell types. (B) Overrepresented ontology groups in 552 genes altered at  $p < 0.05$  and more than 1.2x in both HLF and HPC. (C) Significantly altered matrix genes ( $p < 0.05$ ) have both discordant and concordant change with TBX4 knockout between cell types. HLF and HPC are each normalized to their own wild-type control; HLF are indicated by blue points and arrows, HPC by red. HLF, human lung fibroblasts; HPC, human lung pericytes.



**Data analysis workflow**



**B HLF TBX4 ChIP-seq**



**C HLPC TBX4 ChIP-seq**

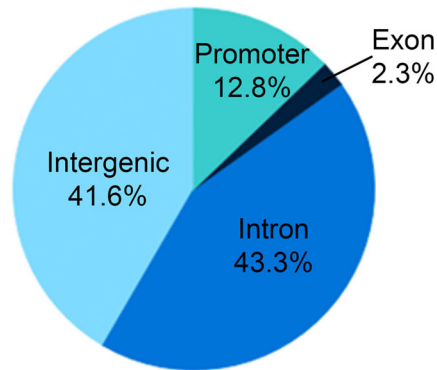


**FIGURE 3** | (A) The workflow of ChIP-seq and following data analysis (B, C) Pie charts show the distribution of TBX4 binding sites in fibroblasts (B) and in pericytes (C) according to peak location across different genomic regions in the human genome. ChIP-seq, chromatin immunoprecipitation sequencing; HLF, human lung fibroblasts; HLPC, human lung pericytes.

**3.5 | TBX4 KD in HLF Reduced Its Migration and Proliferation**

The vascular ECM not only provides mechanical support and maintains vascular wall integrity but also plays a crucial role in mediating cellular adhesion and migration. To investigate the role of TBX4 in ECM-related functions, we knocked down TBX4 in HLF using siRNA, confirming the knockdown at both RNA (Supporting Information: Table 1A) and protein levels (data not shown).

In a migration assay, compared to the control, TBX4 KD in HLF had significantly reduced migration (Figure 5A), with the migration distance decreased 50% compared to that of KD control (Figure 5B).

Additionally, we assessed whether TBX4 KD affects cell proliferation using bromodeoxyuridine (BrdU) incorporation assays. These results showed that TBX4 KD HLF exhibited a lower BrdU incorporation rate, indicating inhibited cell proliferation compared to control (Figure 5C). These migration and

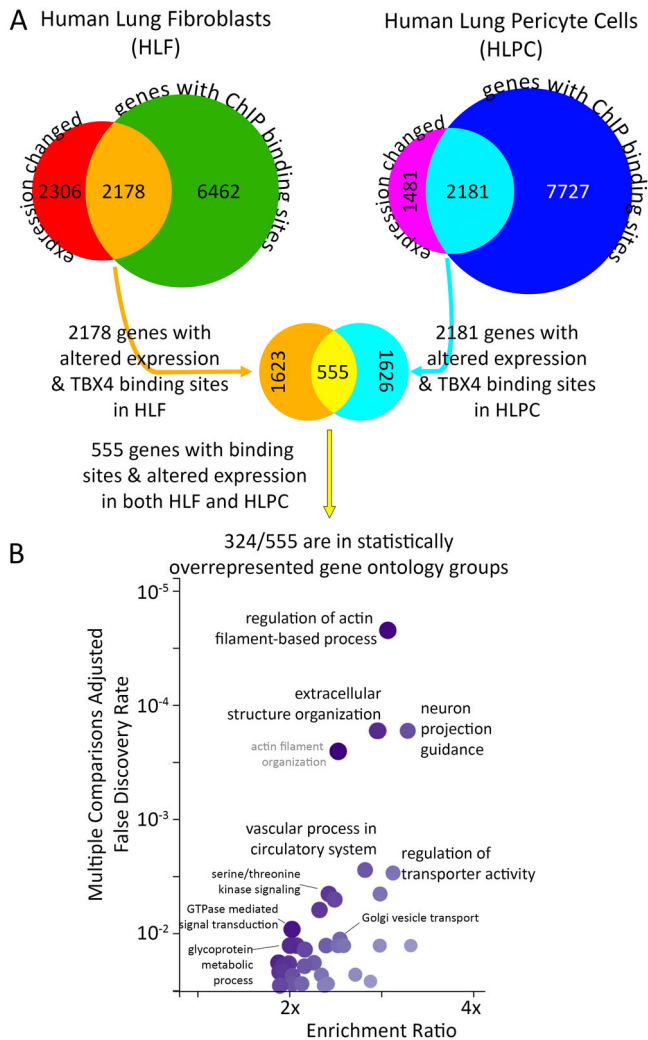


**FIGURE 4** | (A) The workflow strategy for combining results from RNA-seq and TBX4 ChIP-seq carried out in HLF and HLPC from control and TBX4KD. There are 555 genes with altered expression in both cell types, and which contain putative TBX4 binding sites by ChIP-seq. Circle size is proportional to number of genes; colors are arbitrary. (B) Plot of false discovery rate and enrichment ratio for overrepresented gene ontology groups among the 555 genes found in (A) above. ChIP-seq, chromatin immunoprecipitation sequencing; HLF, human lung fibroblasts; HLPC, human lung pericytes.

proliferation functional analyses confirmed that TBX4 positively regulates ECM organization.

## 4 | Discussion

In this study, we aimed to elucidate the molecular mechanisms by which TBX4 functions as a transcription factor in lung mesenchymal cells, specifically focusing on its role in pulmonary vascular development and pathology. By integrating ChIP-Seq and RNA-Seq analyses in HLF and HLPC, we identified direct genomic targets of TBX4 and mapped the downstream transcriptional networks it regulates. Our findings reveal that TBX4 plays a pivotal role in regulating extracellular matrix (ECM) organization, cell migration, and proliferation—processes that are critical for pulmonary

vascular development and may contribute to the pathogenesis of PAH.

Our results confirm that TBX4 expression is predominantly localized to lung mesenchymal cells, specifically fibroblasts and pericytes. This observation is consistent with previous studies and single-cell RNA sequencing data from developing mouse lungs, which show negligible TBX4 expression in epithelial and endothelial cells [28, 29]. By focusing on HLF and HLPC, we demonstrated that TBX4 knockdown significantly alters the expression of thousands of genes in both cell types. Notably, while there was some overlap in the genes and pathways affected, we also observed cell type-specific differences, underscoring the diverse roles of TBX4 in lung mesenchyme.

The ChIP-Seq analysis identified a substantial number of TBX4 binding sites in both HLF and HLPC, indicating widespread genomic occupancy. More than 40% of TBX4 DNA binding peaks in both HLF and HLPC ChIP-seq were located in intergenic regions [30]. This binding pattern is consistent with previously published experiments which employed the human fetal lung fibroblasts IMR-90 for chromatin immunoprecipitation followed by ChIP-seq studies [14].

Integrating our data with the RNA-Seq results allowed us to pinpoint direct TBX4 targets. Webgestalt pathway analysis of these targets revealed that TBX4 regulates several pathways involved in ECM organization, cell motility, and signaling pathways related to small GTP signaling. These data are consistent with previous expression data from an adult normal human lung fibroblast (NHLF) line that indicated that TBX4 was required for cell proliferation and collagen gel contraction capacity [30]. Taken together, these data suggest that TBX4 has a fundamental role in orchestrating the structural and functional components of the lung mesenchymal ECM.

Our functional assays further supported the role of TBX4 in ECM-related processes. TBX4 knockdown in HLF resulted in significantly reduced cell migration and proliferation, highlighting its positive regulatory role in these essential cellular functions. Given that the ECM not only provides structural support but also influences cell behavior and tissue remodeling, these findings suggest that TBX4 may influence pulmonary vascular development and pathology through modulation of ECM components and cell dynamics.

These results enhance our understanding of the molecular mechanisms by which TBX4 contributes to pulmonary vascular development and the pathogenesis of PAH. Rare variants (mutations) in TBX4 are linked to a diverse array of disorders, ranging from PAH and ischiocoxopodopatellar syndrome (ICPPS)/small patella syndrome (SPS) to lethal lung developmental disorders (LLDDs). In developmental models, TBX4 play a crucial role in airway branching during the pseudoglandular stage of lung development. Consistent with TBX4's role in development, a TBX4 inducible knockout mouse model exhibited alveolar simplification and mild PAH at birth [22]. Our study provides evidence that TBX4 directly regulates genes involved in ECM organization and cell motility, offering a potential mechanistic link between TBX4 dysfunction and the vascular abnormalities observed in PAH patients with TBX4 mutations.

**TABLE 1** | Ontology groups significantly overrepresented in genes bound and regulated by TBX4 in human lung fibroblasts and human lung pericyte cells.

GO group	Description	# Genes	FDR
GO:0032970	Regulation of actin filament-based process	34	2.2E-05
GO:0043062	Extracellular structure organization	29	1.7E-04
GO:0097485	Neuron projection guidance	24	1.7E-04
GO:0003018	Vascular process in circulatory system	23	2.8E-03
GO:0032409	Regulation of transporter activity	19	3.0E-03
GO:0007178	Transmembrane receptor protein serine/threonine kinase signaling pathway	27	4.5E-03
GO:0007264	Small GTPase-mediated signal transduction	32	9.3E-03
GO:0048193	Golgi vesicle transport	22	1.3E-02
GO:0009100	Glycoprotein metabolic process	25	1.4E-02
GO:0044772	Mitotic cell cycle phase transition	27	1.8E-02

Abbreviation: FDR, false discovery rate.

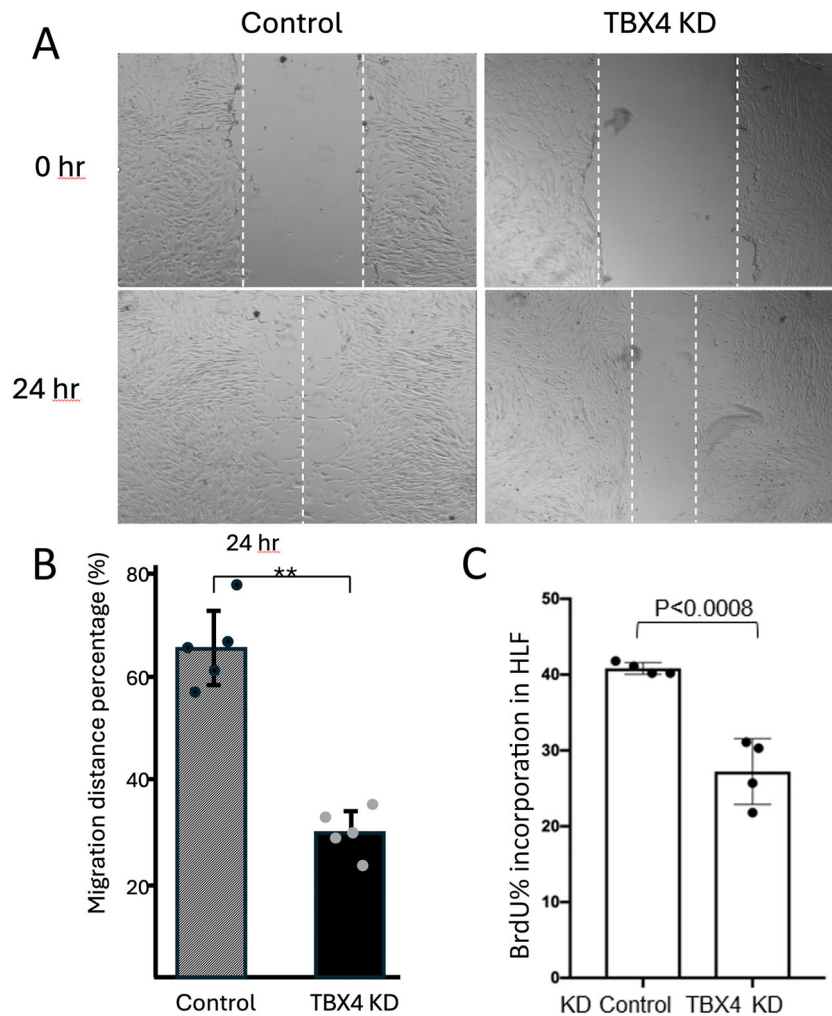


**FIGURE 5** | Migration and BrdU proliferation assays by knocking down TBX4 in HLF. (A) Time-lapse microscopy images of migration of knockdown (KD) control (left panels) and TBX4 KD (right panels) in HLF at 0, 24 h after scratch. The dotted lines define the area lacking cells. (B) Quantification of the migration distance during 24 h. (C) Quantitative analysis of BrdU-positive HLF TBX4 KD control and TBX4 KD cells after incubated with BrdU 48 h. BrdU, bromodeoxyuridine; HLF, human lung fibroblasts.



Moreover, the differential gene regulation observed between HLF and HLPC underscores the cell type-specific functions of TBX4. While some pathways and targets were common to both cell types, others were uniquely regulated, suggesting that TBX4's role may vary depending on the cellular context. This highlights the complexity of TBX4-mediated transcriptional regulation and its potential diverse effects on lung development and disease.

## 5 | Limitations and Future Directions

While our study provides valuable insights into TBX4 function in lung mesenchymal cells, several limitations should be acknowledged. First, our experiments were conducted in vitro using cultured cell lines, which may not fully recapitulate the in vivo environment of the developing or diseased lung. Future studies employing in vivo models, such as conditional TBX4 knockout mice or organoid cultures, would enhance the physiological relevance of our findings. Second, the knockdown of TBX4 achieved in our experiments was partial, and the effects of complete loss of function or overexpression remain to be explored. Understanding the full spectrum of TBX4's activity could reveal additional targets and pathways involved in pulmonary vascular development.

Additionally, our functional assays were limited to cell migration and proliferation. Investigating other cellular processes affected by TBX4, such as differentiation, apoptosis, and responses to hypoxia, could provide a more comprehensive understanding of its role in lung biology. Exploring the interactions between TBX4 and other transcription factors or signaling pathways known to be involved in PAH, such as the BMP-SMAD and Notch pathways, may uncover synergistic mechanisms contributing to disease progression.

Further research is also needed to investigate the impact of specific TBX4 mutations identified in PAH patients. Functional studies examining how these mutations affect TBX4's DNA-binding ability, transcriptional activity, and interaction with co-regulators would provide valuable insights into genotype-phenotype correlations and potential therapeutic targets.

## 6 | Conclusions

In summary, our integrated ChIP-Seq and RNA-Seq analyses demonstrate that TBX4 directly regulates genes involved in ECM organization and cell motility in lung mesenchymal cells. These findings provide a mechanistic basis for the role of TBX4 in pulmonary vascular development and contribute to our understanding of how TBX4 mutations may lead to PAH. By elucidating the downstream targets and pathways regulated by TBX4, our study lays the groundwork for future investigations into therapeutic strategies aimed at modulating TBX4 activity or its downstream effects in pulmonary vascular diseases.

### Author Contributions

Conceptualization: Ying Cai, James West, Eric D. Austin, and Rizwan Hamid. Methodology: Ying Cai, Joy D. Cogan, Lora K. Hedges, Bethany

Nunley, Nick Negretti, and Jennifer M. S. Sucre. Validation: Ying Cai, Ling Yan, Lora K. Hedges, and Bethany Nunley. Formal analysis: James West and Ying Cai. Investigation: Ying Cai, Joy D. Cogan, Lora K. Hedges, Bethany Nunley, Nick Negretti, and Jennifer M. S. Sucre. Data curation: James West and Ying Cai. Writing—original draft preparation: Ying Cai. Writing—review and editing: Ying Cai, Eric D. Austin, Rizwan Hamid, Jennifer M. S. Sucre, and James West. Visualization: James West and Ying Cai. Supervision: James West and Eric D. Austin. Funding acquisition: Eric D. Austin, Rizwan Hamid, and James West.

### Acknowledgments

We thank Dr. Hongkuan Fan (Pathology and Laboratory Medicine, Medical University of South Carolina, Charleston, SC 29425, USA) for providing the human lung pericyte (HLPC) cell line. Funding was provided by NIH P01 HL 108800 (E.D.A.), NIH R01 HL134802 (E.D.A.), NIH R01HL095797 (J.W.) and NIH R01 HL 102020 awards (R.H.), as well as the Cardiovascular Medical Research and Education Fund (CMREF) (E.D.A.).

### Ethics Statement

All the mice utilized in this study were housed at Vanderbilt University Medical Center animal care facility, which is certified by the Association for Assessment and Accreditation of Laboratory Animal Care International. All animal protocols were approved by the Institutional Animal Care and Use Committee at Vanderbilt University Medical Center in compliance with National Institute of Health guidelines.

### Conflicts of Interest

The authors declare no conflicts of interest.

### Data Availability Statement

RNA-seq data is available at Geo (<https://www.ncbi.nlm.nih.gov/geo/>) as accession number GSE273499. Much of the remaining raw data has been included as supplemental figures; other data available on request of the authors.

### Guarantor

James West serves as the submission's guarantor. He takes responsibility for the integrity of the work as a whole, from inception to published article.

### References

1. R. Arora, R. J. Metzger, and V. E. Papaioannou, "Multiple Roles and Interactions of Tbx4 and Tbx5 in Development of the Respiratory System," *PLoS Genetics* 8 (2012): e1002866.
2. F. Soubrier, W. K. Chung, R. Machado, et al., "Genetics and Genomics of Pulmonary Arterial Hypertension," *Journal of the American College of Cardiology* 62 (2013): D13–D21.
3. C. Galambos, M. P. Mullen, J. T. Shieh, et al., "Phenotype Characterisation of TBX4 Mutation and Deletion Carriers With Neonatal and Paediatric Pulmonary Hypertension," *European Respiratory Journal* 54 (2019): 1801965.
4. E. M. H. F. Bongers, P. H. G. Duijf, S. E. M. van Beersum, et al., "Mutations in the Human TBX4 Gene Cause Small Patella Syndrome," *American Journal of Human Genetics* 74 (2004): 1239–1248.
5. K. German, G. H. Deutsch, A. S. Freed, K. M. Dipple, S. Chabra, and J. T. Bennett, "Identification of a Deletion Containing TBX4 in a Neonate With Acinar Dysplasia by Rapid Exome Sequencing," *American Journal of Medical Genetics, Part A* 179 (2019): 842–845.
6. I. Hernandez-Gonzalez, J. Tenorio, J. Palomino-Doza, et al., "Clinical Heterogeneity of Pulmonary Arterial Hypertension Associated With Variants in TBX4," *PLoS One* 15 (2020): e0232216.

7. J. A. Karolak, P. Szafranski, D. Kilner, et al., "Heterozygous CTNNB1 and TBX4 Variants in a Patient With Abnormal Lung Growth, Pulmonary Hypertension, Microcephaly, and Spasticity," *Clinical Genetics* 96 (2019): 366–370.
8. W. S. Kerstjens-Frederikse, E. M. H. F. Bongers, M. T. R. Roofthoof, et al., "TBX4 Mutations (Small Patella Syndrome) Are Associated With Childhood-Onset Pulmonary Arterial Hypertension," *Journal of Medical Genetics* 50 (2013): 500–506.
9. L. A. Naiche and V. E. Papaioannou, "Loss of Tbx4 Blocks Hindlimb Development and Affects Vascularization and Fusion of the Allantois," *Development* 130 (2003): 2681–2693.
10. P. Navas, J. Tenorio, C. A. Quezada, et al., "Análisis De Los Genes BMPR2, TBX4 y KCNK3 Y Correlación Genotipo-Fenotipo En Pacientes Y Familias Españolas Con Hipertensión Arterial Pulmonar," *Revista Española de Cardiología* 69 (2016): 1011–1019.
11. M. Nimmakayalu, H. Major, V. Sheffield, et al., "Microdeletion of 17q22q23.2 Encompassing TBX2 and TBX4 in a Patient With Congenital Microcephaly, Thyroid Duct Cyst, Sensorineural Hearing Loss, and Pulmonary Hypertension," *American Journal of Medical Genetics, Part A* 155A (2011): 418–423.
12. K. Suhrie, N. M. Pajor, S. K. Ahlfeld, et al., "Neonatal Lung Disease Associated With TBX4 Mutations," *Journal of Pediatrics* 206 (2019): 286–292.e1.
13. L. Y. Ying Cai, M. J. Kiehl, J. D. Cogan, et al., "TBX4 Transcription Factor Is a Positive Feedback Regulator of Itself and Phospho-SMAD1/5," *American Journal of Respiratory Cell and Molecular Biology* 64 (2021): 140–143.
14. J. A. Karolak, T. Gambin, P. Szafranski, and P. Stankiewicz, "Potential Interactions Between the TBX4-FGF10 and SHH-FOXF1 Signaling During Human Lung Development Revealed Using Chip-Seq," *Respiratory Research* 22 (2021): 26.
15. G. Tuteja, P. White, J. Schug, and K. H. Kaestner, "Extracting Transcription Factor Targets From Chip-Seq Data," *Nucleic Acids Research* 37 (2009): e113.
16. H. S. Rhee and B. F. Pugh, "Comprehensive Genome-Wide Protein-DNA Interactions Detected at Single-Nucleotide Resolution," *Cell* 147 (2011): 1408–1419.
17. J. M. S. Sucre, D. Wilkinson, P. Vijayaraj, et al., "A Three-Dimensional Human Model of the Fibroblast Activation That Accompanies Bronchopulmonary Dysplasia Identifies Notch-Mediated Pathophysiology," *American Journal of Physiology-Lung Cellular and Molecular Physiology* 310 (2016): L889–L898.
18. N. M. Negretti, E. J. Plosa, J. T. Benjamin, et al., "A Single-Cell Atlas of Mouse Lung Development," *Development* 148 (2021): dev199512.
19. S. Heinz, C. Benner, N. Spann, et al., "Simple Combinations of Lineage-Determining Transcription Factors Prime Cis-Regulatory Elements Required for Macrophage and B Cell Identities," *Molecular Cell* 38 (2010): 576–589.
20. C. Guignabert, J. Aman, S. Bonnet, et al., "Pathology and Pathobiology of Pulmonary Hypertension: Current Insights and Future Directions," *European Respiratory Journal* 64 (2024): 2401095.
21. J. A. Karolak, C. L. Welch, C. Mosimann, et al., "Molecular Function and Contribution of TBX4 in Development and Disease," *American Journal of Respiratory and Critical Care Medicine* 207 (2023): 855–864.
22. G. Maldonado-Velez, E. A. Mickler, T. G. Cook, and M. A. Aldred, "Loss of Tbx4 Affects Postnatal Lung Development and Predisposes to Pulmonary Hypertension," preprint, bioRxiv, September 22, 2024.
23. M. Merkenschlager and D. T. Odom, "CTCF and Cohesin: Linking Gene Regulatory Elements With Their Targets," *Cell* 152 (2013): 1285–1297.
24. F. Spitz and E. E. M. Furlong, "Transcription Factors: From Enhancer Binding to Developmental Control," *Nature Reviews Genetics* 13 (2012): 613–626.
25. R. G. Roeder, "Transcriptional Regulation and the Role of Diverse Coactivators in Animal Cells," *FEBS Letters* 579 (2005): 909–915.
26. C. J. Favre, M. Mancuso, K. Maas, J. W. McLean, P. Baluk, and D. M. McDonald, "Expression of Genes Involved in Vascular Development and Angiogenesis in Endothelial Cells of Adult Lung," *American Journal of Physiology-Heart and Circulatory Physiology* 285 (2003): H1917–H1938.
27. A. Vadivel, R. S. Alphonse, J. J. P. Collins, et al., "The Axonal Guidance Cue Semaphorin 3C Contributes to Alveolar Growth and Repair," *PLoS One* 8 (2013): e67225.
28. T. Xie, J. Liang, N. Liu, et al., "Transcription Factor TBX4 Regulates Myofibroblast Accumulation and Lung Fibrosis," *Journal of Clinical Investigation* 126 (2016): 3063–3079.
29. K. J. Travaglini, A. N. Nabhan, L. Penland, et al., "A Molecular Cell Atlas of the Human Lung From Single-Cell RNA Sequencing," *Nature* 587 (2020): 619–625.
30. M. Horie, N. Miyashita, Y. Mikami, et al., "TBX4 Is Involved in the Super-Enhancer-Driven Transcriptional Programs Underlying Features Specific to Lung Fibroblasts," *American Journal of Physiology-Lung Cellular and Molecular Physiology* 314 (2018): L177–L191.

### Supporting Information

Additional supporting information can be found online in the Supporting Information section.